中國機械工程學刊第四十六卷第一期第 83~90 頁(民國一百一十四年)
Journal of the Chinese Society of Mechanical Engineers, Vol.46, No.1, pp83~90 (2025)

Analysis of the Magnet-Rotating-Type Axial Magnetic Coupler Speed Regulation Performance

Ao Wang*, Yafei Guo*, Jian Wang* and Yutang Qi*

Keywords: permanent magnet (PM), magnet-rotating-type axial magnetic coupler (MAMC), speed regulation model, transfer torque.

ABSTRACT

To solve the current problem of a single magnetic coupler speed regulation method, a permanent magnet (PM) rotatable magnetic coupler structure is proposed, named magnet-rotating-type axial magnetic coupler (MAMC). The MAMC can be speed regulated in three ways: through air gap regulation, rotary regulation, and composite regulation. Then, a test platform of MAMC was built to carry out experimental research on speed regulation model of constant torque load, quadratic rate load and constant power load. The results show that the composite speed regulation method has a wider speed range compared to the air gap speed regulation method under the quadratic rate load speed regulation model. Under the constant torque load and constant power load speed regulation model, the composite speed regulation method not only has a wider speed range but also has a larger transfer torque compared to the air gap speed regulation method.

INTRODUCTION

Magnetic couplers can transfer torque and speed without mechanical contact. It can avoid the friction and wear problems of traditional transmission devices and has the advantages of soft start and overload protection. Therefore, it is widely used in the industrial field of transmission and braking systems (Atallah et al., 2011; Ye et al., 2011).

At present, scholars around the world are more mature in the theoretical study of the magnetic coupler, and the research methods are mainly finite element method (FEM) and analytical method. The FEM is the output results after structural design, material setup, and kinematic constraints in finite element software (Meng et al., 2015; Erasmus et al., 2017). This method requires high computer hardware. The analytical method can be divided into the magnetic equivalent circuit (MEC) method and the layer model method. The equivalent magnetic circuit method is the permanent magnet (PM) is regarded as a magnetic potential, the medium through which the magnetic circuit passes is regarded as magnetoresistance, and a magnetic circuit diagram is established, then combined with Kirchhoff's law an analytical model is established (Wang et al., 2019; Yeo et al., 2019). However, this method has a larger error in larger air gaps (Wang et al., 2018). The layer model method is a combination of field analysis (magnetic fields and eddy current fields) and sub-domain model, where an analytical model is established by Maxwell's equations and boundary conditions are added (Lubin et al., 2017; Wang et al., 2014; Min et al., 2015). This method can solve the problem of large errors at large air gaps (Wang., 2022). These research methods provide a theoretical foundation for the study of magnetic coupler performance.

To improve the transmission performance of magnetic couplers, scholars around the world have innovated their structures. The magnetic field direction of PMs adopts the Halbach arrangement so that the main magnetic circuit has a better magnetizing effect, which in turn improves the transmission torque (Li et al., 2023; Kim et al., 2016). Slotted and embedded higher permeability ferrous material in the conductor sheet (CS) to increase eddy current density on the copper conductor and thus increase drive torque density (Razavi et al., 2006; Dai et al., 2016). Magnetic couplers have a wider speed range in industrial applications while fulfilling a certain drive torque. However, little research has been done on the speed range of axial magnetic couplers. At present, the axial magnetic coupler is only a way to regulate the speed by adjusting the thickness of the air gap between the PM rotor and the CS rotor.

To solve the problem of axial magnetic coupler speed regulation range is narrow. In this paper, a PM rotatable axial magnetic coupler structure is

Paper Received January, 2024. Revised June, 2024. Accepted August, 2024. Author for Correspondence: Ao Wang.

* *School of Mechanical Engineering, Jiangsu University, Zhenjiang, Jiangsu 212013, China.*

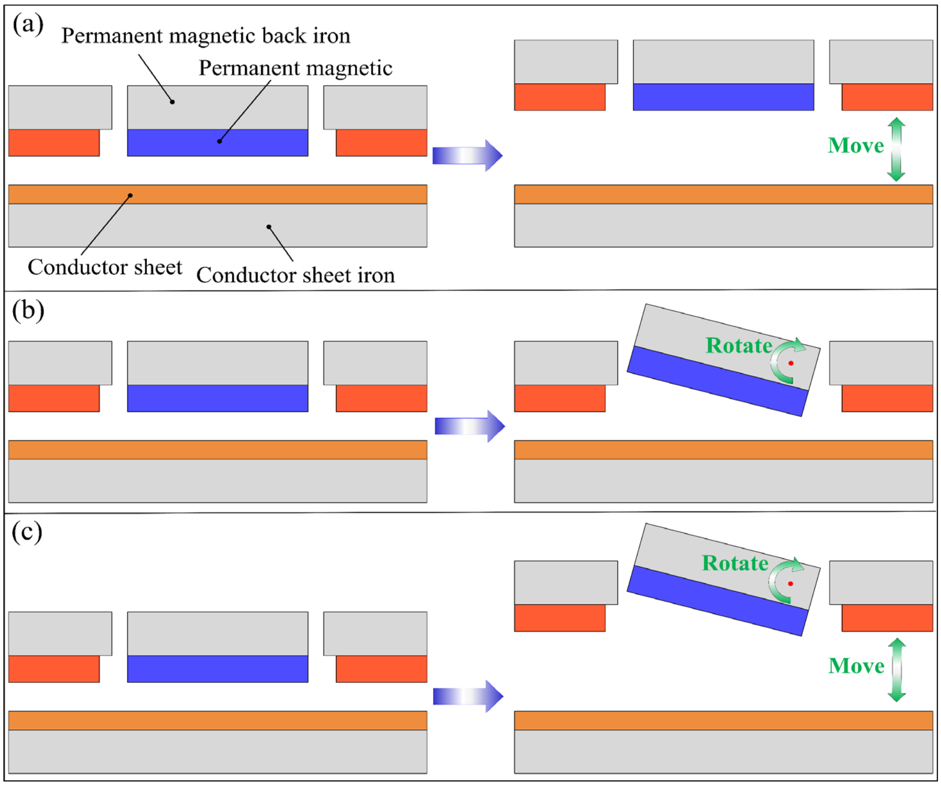

Fig.1. Speed regulation methods of the MAMC. (a) air gap regulation, (b) rotary regulation, (c) composite regulation.

proposed, which can be speed-regulated in three methods: air gap regulation, rotary regulation, and composite regulation. The test bench was built after the prototype was produced. Speed regulation experiments were carried out under the constant torque load, quadratic rate load, and constant torque load speed regulation relationship models.

STRUCTURE DESIGN

Speed regulation method

Fig. 1 shows the three speed regulation methods of MAMC. The first is the air gap regulation. The air gap thickness between the PM rotor and the CS rotor is adjusted, and the magnetic flux density at the CS is changed, so that the transfer torque is changed. Finally, the output rotational speed is changed, realizing the speed regulation function of MAMC. The second type is rotary regulation. The PM and its back iron are rotated at a certain angle to change the effective air gap thickness, the coupled area, and the array of PMs between the PM rotor and the CS rotor, thus the magnetic flux density and the transfer torque at the CS is changed, and thus realizing the regulation of the MAMC rotating speed. The third is the composite regulation. This means the thickness of the air gap between the PM rotor and the CS rotor is adjusted, while the PM and its back iron are rotated at a certain angle to realize the function of speed regulation. The limitation is broken that conventional magnetic couplers can only be used for air gap speed regulation, and diversifying the speed regulation methods.

3-D structure design

Fig. 3 shows the 3-D structural model of MAMC, and its relevant structural parameters are shown in Table 1. Order to ensure that the structural parameters presented in Table 1 are clearly linked to the 3-D structural model for better understanding. Fig. 4 shows the geometrical structure of MAMC, the parameter symbols correspond to Table 1. PMs are uniformly arranged in the circumferential direction, and the magnetic fields of neighboring PMs are in opposite directions. Rotatable PMs have the same magnetic field direction and are fixedly connected to their backing iron. The gear disk engages with the bevel gear, and the bevel gear is coaxial with the back iron of the rotatable PM. The rotated gear shaft rotates the gear disk, and the bevel gear is driven to rotate, and the angle of the rotatable PM is changed to realize the speed regulation function. All rotatable PMs have the same rotation angle.

THEORETICAL ANALYSIS

Derivation process of magnetic induction intensity according to reference (Wang et al., 2018). As shown in Fig. 2, when the rotatable PM rotates at a certain angle θ, the magnetic field line in the air gap changes from a straight line to an arc line. If the minimum radius of the magnetic field line is set to r_1, the maximum radius of the magnetic field line is $(r_1+\tau_m)$, and the magnetoresistance of the air gap can be expressed as

$$R_a=\begin{cases}1\Big/\int_{r_1}^{r_1+\tau_m}\dfrac{\mu_0\omega_m dr}{r\theta} & \theta\neq 0\\[2ex] \dfrac{g}{\mu_0\omega_m\tau_m} & \theta=0\end{cases} \qquad (1)$$

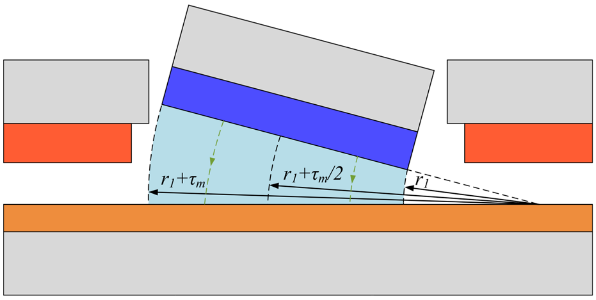

Fig. 2. Air gap flux path between the rotatable PM and the CS.

Derivation formula of air gap magnetic current Φ_g

$$\Phi_g=\frac{V_{pg}}{R_g} \qquad (2)$$

The derivation formula of magnetic induction intensity B_c on CS

$$B_c=\frac{\Phi_g}{\omega_m\tau_m} \qquad (3)$$

In summary, the derivation formula of magnetic induction intensity B_c on CS can be simplified as

$$B_c=\begin{cases}\dfrac{V_{pg}\int_{r_1}^{r_1+\tau_m}\dfrac{\mu_0\omega_m dr}{r\theta}}{\omega_m\tau_m} & \theta\neq 0\\[2ex] \dfrac{V_{pg}\mu_0}{g} & \theta=0\end{cases} \qquad (4)$$

From (4), as the rotation angle of the rotatable PM increases, the radius of the magnetic field line decreases. Because it is very difficult to calculate the radius of the magnetic field line, it is difficult to know how the magnetic induction intensity B_c changes on CS, so it is necessary to explore through experiments.

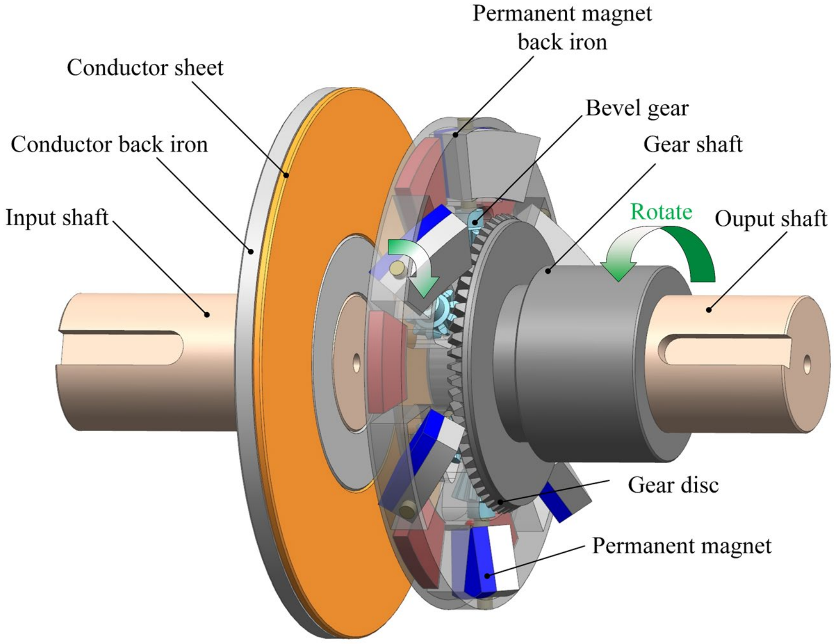

Fig. 3. 3-D structure of MAMC.

Table 1. Specifications of the MAMC.

Parameter	Value	Parameter	Value
Number of PM pole pairs	6	Thickness of the CS, t_c	5 mm
Angle of pole-arc, θ_m	25°	Thickness of the PM back iron, t_{mi}	12 mm
Inner radius of the PM, r_{m1}	85 mm	Thickness of the CS back iron, t_{ci}	10 mm
Outer radius of the PM, r_{m2}	120 mm	Relative permeability of the PM	1.099
Thickness of the PM, t_m	8 mm	Relative permeability of back iron	2000
Inside radius of the CS, r_{c1}	65 mm	Coercive force of the PM	−868 kA/m
Outside radius of the CS, r_{c2}	140 mm	Conductivity of the CS	5.7×10^7 S/m

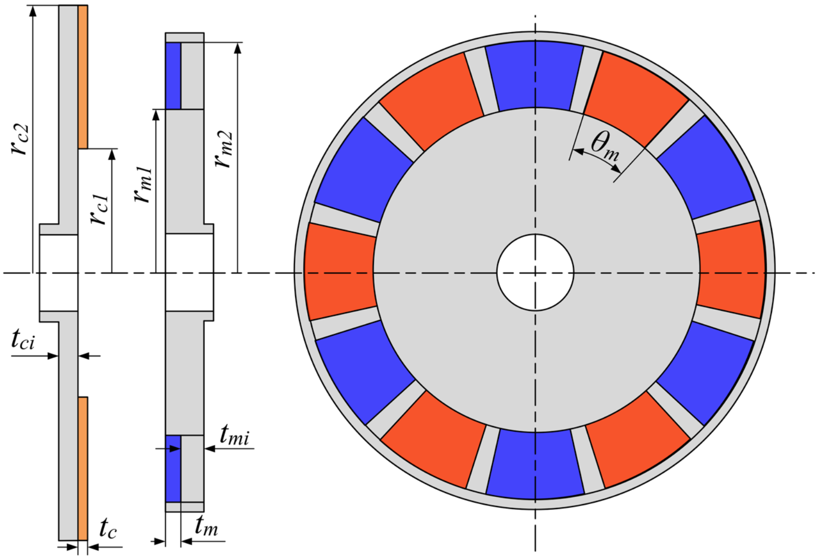

Fig. 4. Geometrical structure of MAMC.

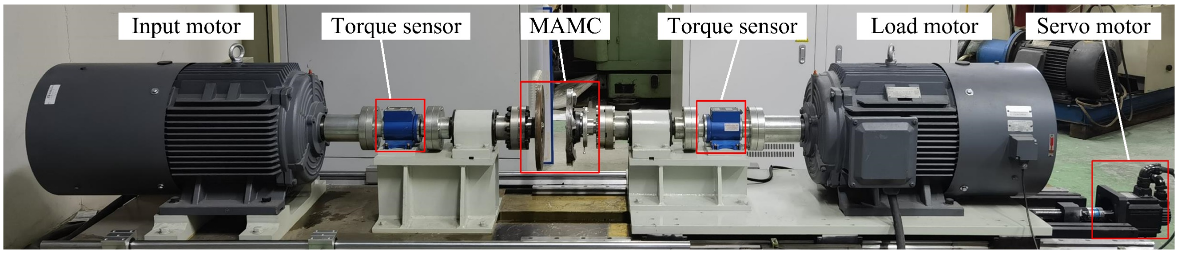

Fig. 5. Experimental platform of the testing system.

EXPERIMENTAL TEST

Experimental platform

Fig. 5 shows the magnetic coupler experimental platform, which includes input motor, torque sensor, MAMC, load motor, and servo motor. The role of the input motor is to control the input speed, the role of the input side torque sensor is to record the input torque data in real time, the role of the output side torque sensor is to record the output torque data in real time, the role of the load motor is to control the output speed, the role of the servo motor is to regulation the air gap thickness between the PM rotor and the CS rotor.

Keep the position of the input side stationary and adjust the position of the output side with the servo motor so that the air gap between PM rotor and CS rotor is 4 mm. Keep the speed of the input motor constant 1200 rpm, the initial speed of the output motor is consistent with the input speed, and the speed decreases by 10 rpm step. The computer collects the torque data recorded by the torque sensor under different output speeds. Repeat the above experimental steps to record the experimental data when the air gap is 8 mm and the air gap thickness is 4 mm and 8 mm, respectively, when the angle of the rotatable PM is 30°.

Table 2. Parameter of experiment

Parameter	Value
Input rotate speed	1200 rpm
Air gap thickness	4 mm and 8 mm
Rotation angle of the rotatable PM	0°and 30°

Speed regulation relationship model

For conveyor belts and mixers, whose load torque is constant, the torque balance equation at the steady state of the MAMC

$$T_m = T_{ct} = C \tag{5}$$

where T_m is the output torque of the MAMC, T_{ct} is the constant load torque, and C is the constant value.

For fans and pumps, whose load torque is quadratically related to the output speed, the torque balance equation at the steady state of the MAMC

$$T_m = T_{cq} = kn_m^2 \tag{6}$$

where T_{cq} is the load torque at the quadratic rate, k is the quadratic rate coefficient, n_m is the output speed.

For rolling mill and paper winding machines, whose power is constant and the load torque is inversely proportional to the output speed, the torque balance equation at the steady state of the MAMC

$$T_m = T_{cp} = \frac{9550P}{n_m} = \frac{9550C_p}{n_m} \tag{7}$$

where T_{cp} is the load torque at constant power, P is the constant power, C_p is the constant value.

ANALYSIS OF RESULTS

Mechanical characteristic

As shown in Fig. 6, the mechanical characteristic curve of MAMC under different air gap thicknesses and PMs rotation angles. The inflection points of the mechanical characteristic curve under different speed regulation parameters correspond to consistent output speeds. The transfer torque reaches its maximum value when the output speed is 860 rpm. It shows that the MAMC has the same critical speed for different speed regulation parameters. The maximum torque of the MAMC is 52 N·m when the air gap thickness and PM rotation angle are 4 mm and 0°. The maximum torque of the MAMC decreases with the increase of air gap thickness and PM rotation angle.

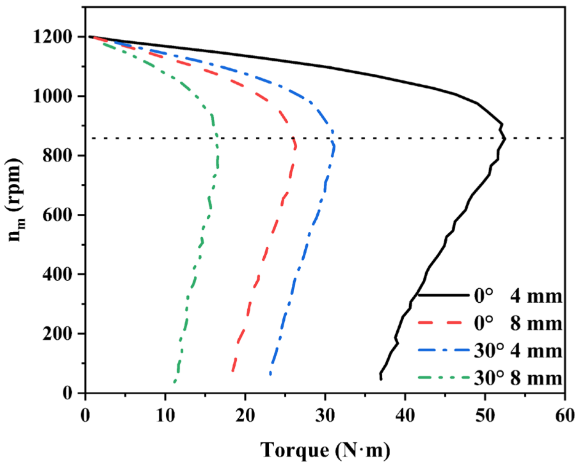

Fig. 6. The mechanical characteristic curve of the MAMC.

Speed regulation curves

Fig 7 is the speed regulation curves of the MAMC. For stable operation of the MAMC, it is necessary to determine its operating speed range under different speed regulation relationship models (Li et al., 2012). (1) The load curve must have an intersection with the mechanical characteristic curve. (2) At the intersection of the curves, the inverse of the load curve slope is greater than the inverse of the mechanical characteristic curve slope at that point. Therefore, the inflection point of the mechanical characteristic curve is the critical point for adjustable speed for constant torque load and constant power load conditions. When the output speed is lower than the critical speed, the MAMC will not be able to operate stably. For quadratic rate loading conditions, all intersection points are normal operating points, independent of critical speeds.

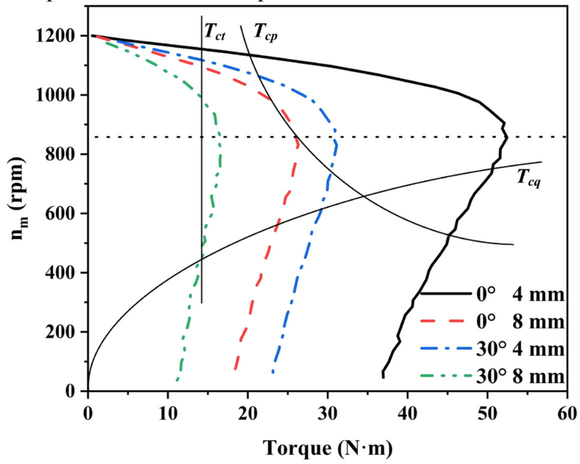

Fig. 7. Speed regulation curves of the MAMC.

Constant torque load speed range curves

Fig. 8 shows the speed range curves of the three speed regulation methods under different load torque values. As the load torque increases, the speed range that can be stabilized by the three speed regulation modes all increase first and then decrease. When the air gap thickness of the MAMC is 8 mm and the PM rotation angle is 30°, the maximum output torque is 16.7 N·m.

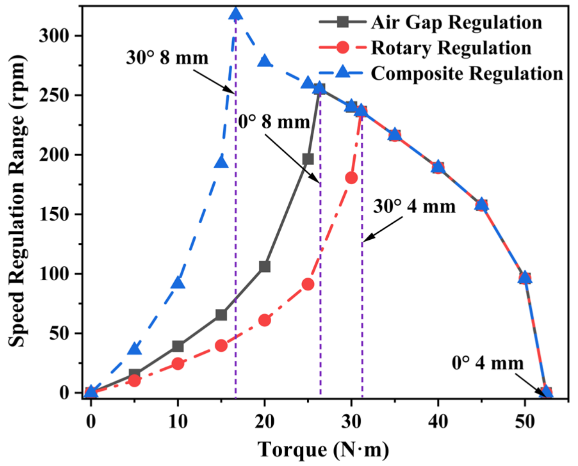

Fig. 8. Speed regulation range of three speed regulation methods under different load torques

At this point, the composite speed regulation method achieves the widest speed range of 0-317.5 rpm, which is much wider than the air gap speed range and the rotary speed range. When the air gap thickness of the MAMC is 8 mm and the PM rotation angle is 0°, the maximum output torque is 26.3 N·m. At this point, the air gap speed regulation method reaches the widest speed range of 0-255.2 rpm, which is the same as the composite speed range and wider than the rotary speed range. When the air gap thickness of the MAMC is 4 mm and the angle of rotation of the PM is 30°, the maximum output torque is 31.1 N·m. At this point, the rotary speed regulation mode reaches the widest speed range of 0-236.4 rpm, and the three speed regulation modes can operate in the same stable speed range. When the air gap thickness of the MAMC is 4 mm and the permanent magnet rotation angle is 0°, the maximum output torque is 52.4 N·m. At this point, the MAMC can only operate at critical speed and cannot be regulated speed. Under the constant torque speed regulation model, the composite speed regulation has a wider speed range compared to the air gap speed regulation.

Quadratic rate load speed range curves

Fig. 9 shows the speed range curves of the three speed regulation methods under different quadratic rate loads. As the torque coefficient increases, the speed range that can be stabilized by the three speed regulation modes all increase first and then decrease. The speed range for stable operation is always wider in the composite mode than in the air gap and rotary modes. When the torque coefficient is 5.1×10^{-5}, the composite speed regulation mode achieves the widest speed range of 0-445 rpm. When the torque coefficient is 6.2×10^{-5} the air gap speed regulation method reaches the widest speed range of 0-284.7 rpm. When the torque coefficient is 6.3×10^{-5} the composite speed regulation method reaches the widest speed range of 0-218.2 rpm. It can be seen that under the quadratic rate speed model, the composite speed regulation has a wider speed range compared to the air gap speed regulation.

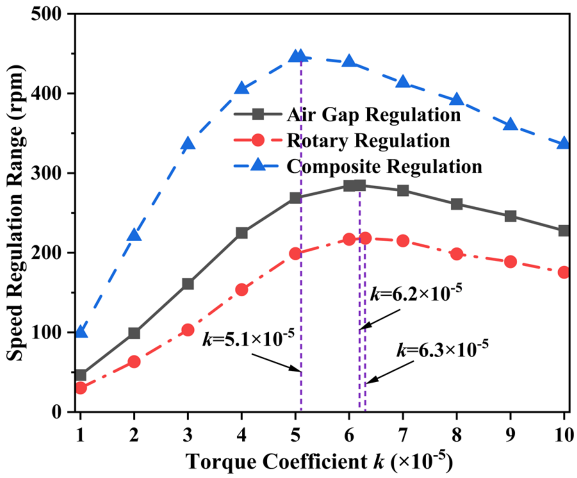

Fig. 9. Speed regulation range of three speed regulation methods under different torque coefficients.

Constant power load speed range curves

Fig. 10 shows the speed range curves of the three speed regulation methods under different power values. Similar to constant torque speed regulation, as the power value increases, the speed range that can be stabilized by the three speed regulation methods all increase first and then decrease. When the air gap thickness of the MAMC is 8 mm and the PM rotation angle is 30°, the maximum output power is 1.5 kW. At this point, the composite speed regulation method achieves the widest speed range of 0-302.7 rpm, which is much wider than the air gap speed range and the rotary speed range. When the air gap thickness of the MAMC is 8 mm and the PM rotation angle is 0°, the maximum output power is 2.37 kW. At this point, the air gap speed regulation method reaches the widest speed range of 0-278.1 rpm, which is the same as the composite speed range and wider than the rotary speed range. When the air gap thickness of the MAMC is 4 mm and the PM rotation angle is 30°, the maximum output power is 2.9 kW. At this point, the rotary speed regulation mode reaches the widest speed range of 0-260.1 rpm, and the three speed regulation modes can operate in the same stable speed range. When the air gap thickness of the MAMC is 4 mm and the permanent magnet rotation angle is 0°, the maximum output power is 4.72 kW. At this point, the MAMC can only operate at critical speed and cannot be regulated speed. Under the constant power speed regulation model, the composite speed regulation has a wider speed range compared to the air gap speed regulation.

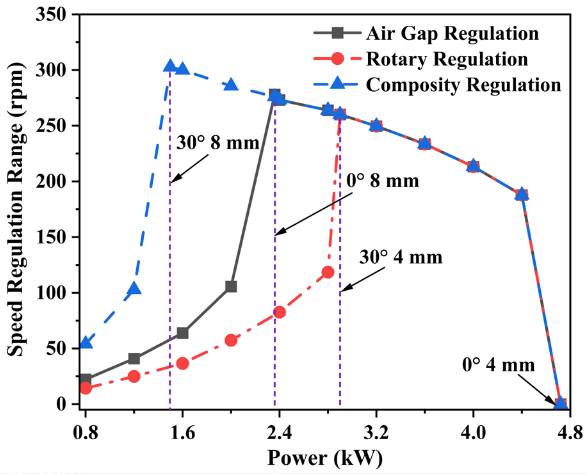

Fig. 10. Speed regulation range of three speed regulation methods under different power values

It should be noted that when the rotating angle of the rotatable PM is 0° and only the air gap speed regulation method is used to speed the MAMC, there is no difference between the MAMC and the traditional magnetic coupler. Therefore, the rotatable PM can be used as a traditional magnetic coupler when the rotation angle is 0°. Compared with the traditional magnetic coupler, the MAMC has a wider speed range when the compound speed regulation method is used to speed the MAMC.

CONCLUSIONS

The magnetic coupler is a non-physical contact regulatable speed transmission device, which is widely favored by industrial fields. In this paper, a permanent magnet rotatable magnetic coupler is invented and its speed regulation characteristics are investigated. The following conclusions can be reached:

(1) The MAMC has three kinds of speed regulation modes: air gap speed regulation, rotary speed regulation, and composite speed regulation. The MAMC breaks the limitation of conventional magnetic couplers that can only be used for air gap speed regulation and diversifies the speed regulation modes.

(2) Under the quadratic rate speed regulation model, the composite speed regulation method has a wider speed regulation range compared to air gap speed regulation. Under the constant torque and constant power speed regulation model, the composite speed regulation not only has a wider speed range but also has a larger transfer torque, compared with the air gap speed regulation.

The MAMC has a promising future in the industry.

REFERENCES

Atallah, K., and Wang, J., “A brushless permanent magnet machine with integrated differential,” *IEEE Trans. Magn.*, Vol. 47, No. 10, pp. 4246-4249, (2011).

Ye, L.Z., Li, D.S., Ma, Y.J., and Jiao, B.F., “Design and performance of a water-cooled permanent magnet retarder for heavy vehicles,” *IEEE Trans. Energy Convers.*, Vol. 26, No. 3, pp. 953-958 (2011).

Meng, Z., Zhu, Z., and Sun, Y., “3-D analysis for the torque of permanent magnet coupler,” *IEEE Trans. Magn.*, Vol. 51, No. 4, No. 8002008 (2015).

Erasmus A.S., and Kamper, M.J., “Computationally efficient analysis of double PM-rotor radial-flux eddy current couplers,” *IEEE Trans. Ind. Appl.*, Vol. 53, No. 4, pp. 3519-3527 (2017).

Wang, S., Guo, Y., Li, D-Y., and Su, C., “Modelling and experimental research on the equivalent magnetic circuit network of hybrid magnetic couplers considering the magnetic leakage effect,” *IET Electr. Power Appl.*, Vol. 13, No. 9, pp. 1413-1421 (2019).

Yeo, H-K., Lim, D-K., and Jung, H-K., “Magnetic equivalent circuit model considering the overhang structure of an interior permanent-magnet machine,” *IEEE Trans. Magn.*, Vol. 55, No. 6, No. 8201404 (2019).

Wang, J., and Zhu, J., “A simple method for performance prediction of permanent magnet eddy current couplings using a new magnetic equivalent circuit model,” *IEEE Trans. Ind. Electron.*, Vol. 65, No. 3, pp. 2487-2495 (2018).

Lubin, T., and Rezzoug, A., “Improved 3-D analytical model for axial-flux eddy-current couplings with curvature effects,” *IEEE Trans. Magn.*, Vol. 53, No. 9, No. 8002409 (2017).

Wang, J., Lin, H., Fang, S., and Huang, Y., “A general analytical model of permanent magnet eddy current couplings,” *IEEE Trans. Magn.*, Vol. 50, No. 1, No. 8000109 (2014).

Min, K-C., Choi, J-Y., Kim, J-M., Cho, H-W., and Jang, S-M., “Eddy current loss analysis of noncontact magnetic device with permanent magnets based on analytical field calculations,” *IEEE Trans. Magn.*, Vol. 51, No. 11, No. 8110304 (2015).

Wang, J., “A generic 3-D analytical model of permanent magnet eddy-current couplings using a magnetic vector potential formulation,” *IEEE Trans. Ind. Electron.*, Vol. 69, No. 1, pp. 663-672 (2022).

Li, D., Wang, S., Guo, Y., and Ma, X., “Modeling and Experimental Study of Halbach Array Magnetic Coupler,” *KSCE J. Civ. Eng.*, Vol. 27, No. 1, pp. 261-269 (2023).

Kim, C., and Choi, J., “Parametric analysis of tubular-type linear magnetic couplings with halbach array magnetized permanent magnet by using analytical force calculation,” *J. Magn.*, Vol. 21, No. 1, pp. 110-114 (2016).

Razavi, H.K., and Lamperth, M.U., “Eddy-current coupling with slotted conductor disk,” *IEEE Trans. Magn.*, Vol. 42, No. 3, pp. 405-410 (2006).

Dai, X., Liang, Q., Cao, J., Long, Y., Mo, J., and Wang, S., “Analytical modeling of axial-flux permanent magnet eddy current couplings with a slotted conductor topology” *IEEE Trans. Magn.*, Vol. 52, No. 5, No. 8000315 (2016).

Li, F.H., and Wang, Y., *Fundamentals of Electric Motors and Drags*, Tsinghua University Press, Beijing (2012).

磁體旋轉型磁力耦合器調速效能分析

汪奥 郭亞飛 王劍 戚玉堂
江蘇大學機械工程學院

摘要

針對現時磁力耦合器調速管道單一問題，提出一種永磁體可旋轉的磁力耦合器結構，命名為磁體旋轉型磁力耦合器。 磁體旋轉型磁力耦合器可通過氣隙調節、旋轉調節和複合調節三種調速管道。

生產磁體旋轉型磁力耦合器樣件，搭建磁體旋轉型磁力耦合器測試平臺，開展恒轉矩負載、二次方率負載和恒功率負載調速模型實驗研究。 結果表明，二次方率負載調速模型下，相對於氣隙調速管道，複合調速管道具有更寬的調速範圍。 恒轉矩負載和恒功率負載調速模型下，相對於氣隙調速管道，複合調速管道不但具有更寬的調速範圍，而且具有更大的傳遞轉矩。